MECE E3028 Mechanical Engineering Laboratory II
Professor Qiao Lin
Spring 2022

Experiment E3: Air Compressor

LABORATORY REPORT

Lab Group 12

Axel Ortega

Bruno Rergis

Anton Deti

Arlene Diaz

Christine Zou

Ashton Buchanan

Samuel Adeniyi

Columbia University
Department of Mechanical Engineering

March 22, 2022

Contents

Acknowledgements

Thanks to Professor Qiao Lin, as well as TAs Kechun Wen and Wenting Dai for their guidance and support throughout the experiment.

Abstract

Although all compressors share the same goal to compress a given volume of gas and increasing its pressure, each contain their own unique abilities. This particular experiment characterizes a single-staged, reciprocating air compressor - otherwise known as a piston compressor - using nozzles of different diameters. It is shown that the air compressor is well represented by a real thermodynamic cycle. This differs from that of an ideal cycle as the air compression and expansion processes are not adiabatic and not reversible, while the air intake and delivery processes are neither isobaric nor isothermal. Entropy further contributes to the irregularities present in the characterization of the air compressor relative to the real thermodynamic cycle. Although the results of the characterization are mostly consistent with the expected values of those of a real air compressor - and thus a real thermodynamic cycle - the experiment demonstrated flaws and thus high levels of error are present, particularly with regards to the mass flow rates.

List of Figures

List of Tables

1 Introduction

Air compressors are found in a wide range of environments because of their even wider range of applications. Everywhere from gas station tire pumps to refrigerators at home have air compressors. There are infinite jobs an air compressor can do but some of the main ones include: filling objects up with air, pressure washing, yard work, and generally powering pneumatic tools. The reason air compressors are used so often for day-to-day activities is because not a lot of work needs to be put in by the user for work to be done and they're very safe tools.

Air compressors use four core processes to successfully compress air to maintain a high internal pressure. The air compressor itself is made of a piston or set of pistons, a receiving tank, and a nozzle. These parts work together to capture, compress, and store air until it needs to be released at a high pressure.

Studying air compressors is important because of their endless array of applications. Their ability to generate high pressure air onsite safely and quickly is extremely useful. As such, there will never be a need to stop studying their cycles to continue to create the most efficient air compressor.

2 Theory

2.1 Ideal Thermodynamic Cycle

An ideal thermodynamic cycle is a simplified closed cycle that analyzes the compression, combustion, and expansion process in an engine with a focus on extraction of work from combustion of the fuel-air mixture (1). In an air compressor - a mechanical device that compresses gases to high pressures - a thermodynamic cycle is used to generate high pressure air(2). The ideal thermodynamic cycle consists of four processes, as shown in the diagram in Fig. 1 (2). These processes depend on the movement of the piston within the air compressor, as shown by the schematic in Fig. 2 (3). In an ideal thermodynamic cycle, friction and heat losses are negligible (2).

From state 4 to state 1, constant pressure and constant temperature intake occurs as the piston, which is initally set at the bottom dead center (BDC) with open valves, draws in ambient air (3). The intake and outlet valves are then closed. From state 1 to 2, isentropic compression occurs, as the piston moves upward and decreases the volume of the compression chamber (and, in turn, compresses the gas)(3). From state 2 to state 3, constant pressure and constant temperature delivery takes place, as the piston continues to move upward at this state with the outlet valve open delivering air; the air is delivered to the receiver (3). Once the piston reaches the top dead center after delivering the available air to the receiver, isentropic expansion occurs from state 3 to state 4 (3). During this process, the piston begins to move downward with the valve leading to the receiver being closed to prevent backflow (3). After the air expands to a certain amount as the piston moves downward, the inlet value is opened for the piston to draw ambient air again and repeat the cycle (3).

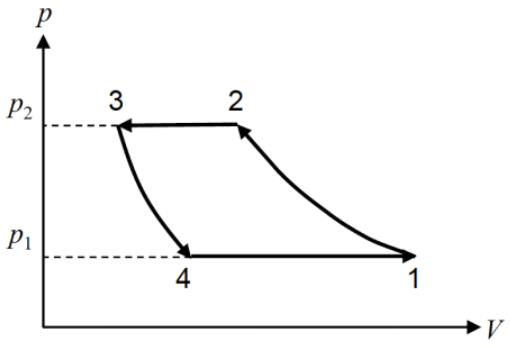

Figure 1: Ideal Thermodynamic Cycle

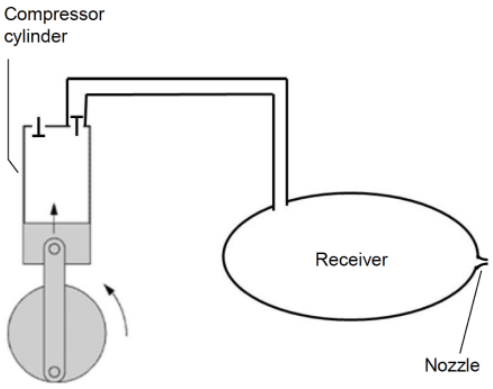

Figure 2: Piston Movement within Compressor

2.2 Real Thermodynamic Cycle

As opposed to the ideal thermodynamic cycle, a real thermodynamic cycle does not operate under constant and reversible conditions (3). This more appropriately represents the operation of the real-world air compressor used in this experiment. This cycle can be seen by the solid-line loop in Fig. 3 (3). The ideal cycle is shown in the dotted line for comparison. The work done on the gas is much larger than the work from the ideal model, as the real compressor must overcome effects due to friction.

From state 4 to state 1, the compressor intakes non-isobaric and non-isothermal air (3). From state 1 to state 2, the air compressor undergoes polytropic compression (3). From state 2 to state 3, non-isobaric and non-isothermal air delivery occurs (3). From state 3 to state 4, polytropic expansion occurs (3). The piston in the compressor moves similarly as that of the ideal cycle, except it no longer operates under adiabatic, isothermal, and isobaric conditions. Overall this requires more work from the air compressor and leads to non-idealized pressures.

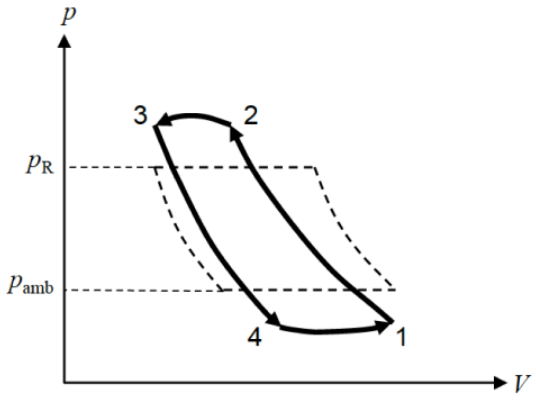

Figure 3: Real Thermodynamic Cycle in an Air Compressor

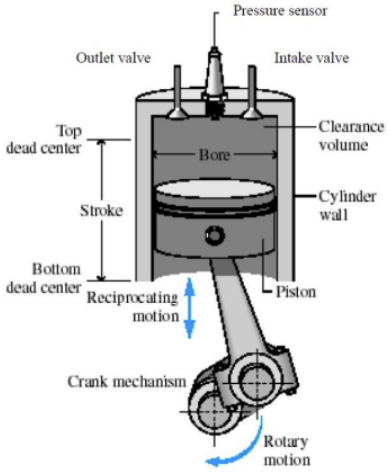

Figure 4: Piston in an air compressor

2.3 Compressor Characteristics

Characteristics of the air compressor can be determined using the values of the pressure and temperature of the air within the compressor at any of the four stages within the cycle in addition to using the isobaric, isothermal, and isentropic relations that govern the thermodynamic cycle within.

2.3.1 Power Input, Power Output, and Power Efficiency of the Motor

Using the calibration curve for an air compressor motor in Fig. 9 from Appendix A.1, the power input P_{in}, power output P_{out}, and power efficiency of the motor η_{motor} are found by Eq. 31, Eq. 32, and Eq. 33.

2.3.2 Determining Operational Parameters

Using the **ideal cycle**, various operational parameters including density, pressure, temperature, and volume can be found. At state 1, the volume, pressure, temperature, and density parameters are $V_1 = V_{BDC}$, $p_1 = p_{amb}$, $T_1 = T_{amb}$, and ρ respectively (2). Due to the isentropic compression between states 1 and 2, the pressure, temperature, and density increase (2). The pressure at state 2 is found to be $p_2 = p_R$, where p_R denotes the pressure at the receiver (tank) (2). T_2, ρ_2, and V_2 are found through isentropic relations (2). At state 3, the pressure, temperature and density are found as $p_3 = p_2$, $T_3 = T_2$, and $\rho_3 = \rho_2$, respectively (2). By isentropic relations again, the parameters at state 4 are found to be $p_4 = p_1$, $T_4 = T_1$, and $\rho_4 = \rho_1$ (2).

2.3.3 Identifying Choked vs. Non-choked Flows

To identify whether the flow is **choked**, the following condition must be satisfied:

$$\frac{p_{amb}}{p_R} \geq 0.528 \tag{1}$$

This denotes that the ratio of ambient pressure to pressure in the receiver tank must be greater than or equal to 0.528 (2). Note that this ratio is specific to air. If this condition is met, then the nozzle pressure is determined by Eq. 2 (2).

$$p_n = p_R \left(\frac{2}{\gamma + 1} \right)^{\gamma/(\gamma-1)} \tag{2}$$

For a **non-choked flow**, the ratio must be less than 0.528 (2). If this is the case, then the nozzle pressure is equivalent to ambient pressure shown in Eq. 3 (2).

$$p_n = p_{amb} \tag{3}$$

2.3.4 Mass Flow Rate

For a one-dimensional steady isentropic flow of a perfect gas (2), the mass flow rate is given by Eq. 4.

$$\dot{m} = \frac{p_R A}{(RT_R)^{1/2}} \left[\frac{2\gamma}{\gamma - 1} \left(\frac{p_n}{p_R} \right)^{2/\gamma} \left(1 - \left(\frac{p_n}{p_R} \right)^{(\gamma-1)/\gamma} \right) \right]^{1/2} \tag{4}$$

The mass flow rate from Eq. 4 can be simplified for a choked flow by substituting the nozzle pressure from Eq. 2 (2). This yields Eq. 5 (2).

$$\dot{m} = \gamma^{\frac{1}{2}} \left(\frac{2}{\gamma + 1} \right)^{\frac{\gamma+1}{2(\gamma-1)}} \frac{p_R A}{(RT_R)^{1/2}} \tag{5}$$

2.3.5 Work and Power of Compression

Based on Fig. 1, the **work done on air by the compressor per cycle** can be found by calculating the area of the shape under the PV diagram (2) (2). This is determined by using Eq. 6, where p denotes pressure and dV denotes volume.

$$W = \int_{cycle} -p dV \tag{6}$$

By evaluating Eq. 6 across the cycle from Fig. 1, it can be further expanded into Eq. 7.

$$W = \frac{\gamma}{\gamma - 1} p_1 \left(V_1 - V_4 \right) \left[\left(\frac{p_2}{p_1} \right)^{\frac{\gamma-1}{\gamma}} - 1 \right] \tag{7}$$

The mass of air processed per cycle is denoted by Eq. 8 (2).

$$m = \rho_2 V_2 - \rho_3 V_3 = \rho_1 V_1 - \rho_4 V_4 \tag{8}$$

By dividing the work per cycle by the mass of air processed per cycle, the **work of compression per unit mass per cycle** can be found in Eq. 9 (2).

$$w = \frac{W}{m} \tag{9}$$

The **steady-state power of compression** is given by Eq. 10 (2). Note that $\dot{m}$ represents the steady state flowrate through the compressor and τ is the time per cycle.

$$\dot{W} = \frac{mw}{\tau} = \dot{m}w \tag{10}$$

When considering the isothermal processes between states 2 and 3 and states 4 and 1 from Fig. 1, $p_3 = p_2$ and $T_3 = T_2$, which also implies $\rho_3 = \rho_2$. Similarly, $p_4 = p_1$ and $T_4 = T_1$, which also implies $\rho_4 = \rho_1$ (2). By substituting these relationships into Eq. 8, the work of compression per unit mass per cycle and steady-state power are found by Eq. 11 and Eq. 10, respectively.

$$w = \frac{\gamma}{\gamma - 1} p_1 \left(\frac{p_1}{\rho_1}\right) \left[\left(\frac{p_2}{p_1}\right)^{\frac{\gamma-1}{\gamma}} - 1\right] \tag{11}$$

2.3.6 Heat Loss

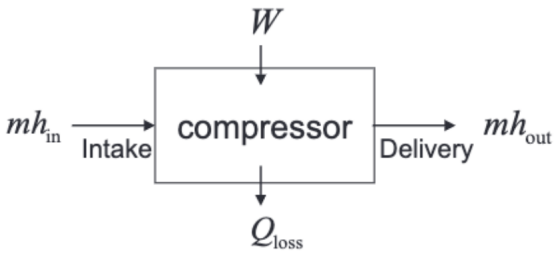

Figure 5: Schematic of Control Volume Enclosing Compressor

Based on Fig. 5 and the first law of thermodynamics, the **total heat loss from air to ambient** can be found using Eq. 12 (2).

$$W - Q_{loss} = mh_{out} - mh_{in} \tag{12}$$

where mh_{in} is the total enthalpy of air taken in, mh_{out} is the total enthalpy of air discharged, W is the total work done by the piston on air, and Q_{loss} is the heat loss from ambient (2). By the same law, it also follows that:

$$\dot{W} - \dot{Q}_{loss} = \dot{m}h_{out} - \dot{m}h_{in} \tag{13}$$

By rearranging Eq 13, the **rate of heat loss from air to ambient** is given by Eq. 14.

$$\dot{Q}_{loss} = \dot{W} - \dot{m}\Delta h \tag{14}$$

The change in enthalpy Δh is given by Eq. 15 (4):

$$\Delta h = c_p \left(T_{outlet} - T_{inlet}\right) \tag{15}$$

where the specifc heat capacity c_p is multiplied by the change in temperature.

The rate of heat loss from a cylindrical surface to the ambient is given by the convention heat transfer model in Eq. 16 (3).

$$\dot{Q} = hA \left(T_{surf} - T_{amb}\right), \tag{16}$$

where A is the total external surface area of the cylinder, T_{surf} is the average temperature of the cylinder surface, T_{amb} is the ambient temperature, and h is the convection heat transfer coefficient (3). By rearranging this equation, a value for the **heat transfer coefficient** h can be found using Eq. 17.

$$h = \frac{\dot{Q}}{A \left(T_{surf} - T_{amb}\right)} \tag{17}$$

2.3.7 Clearance Ratio

The clearance ratio C is found by Eq. 18 (2).

$$C = \frac{V_3}{V_1 - V_3} \tag{18}$$

Using Eq. 18, the volumes at state 1 and state 3 can be determined. These can be seen by Eq. 19 and Eq. 20.

$$V_1 = (V_1 - V_3) + V_3 = (1 + C)V_{stroke} \tag{19}$$

$$V_3 = C(V_1 - V_3) = CV_{stroke} \tag{20}$$

where V_{stroke} is $V_1 - V_3$.

2.4 Efficiencies

2.4.1 Volumetric Efficiency

The volumetric efficiency represents the effectiveness of the compressor cylinder to compress gas. This efficiency is denoted by Eq. 21 (2).

$$\eta_V = \frac{V_1 - V_4}{V_1 - V_3} \tag{21}$$

By isentropic expansion from state 3 to state 4, it follows that:

$$\frac{V_4}{V_3} = \left(\frac{p_2}{p_1}\right)^{\frac{1}{\gamma}}$$

Then, by applying this condition and the clearance ratio in Eq. 18 to Eq. 21, the volumetric efficiency can be rewritten in terms of the pressure and clearance ratios. This is derived in Eq. 22 (2).

$$\eta_V = 1 + C - C\left(\frac{p_2}{p_1}\right)^{\frac{1}{\gamma}} \tag{22}$$

This can further be simplified to Eq. 23.

$$\eta_v = 1 - C\left[\left(\frac{p_2}{p_1}\right)^{(1/\gamma)} - 1\right] \tag{23}$$

Alternatively, volumetric efficiency can be expressed in terms of flowrates as seen by Eq. 24 (2).

$$\eta_V = \frac{\dot{m}}{\dot{m}_{\text{stroke}}} \tag{24}$$

where the theoretical flow rate of the piston stroke is given by Eq. 25 (2).

$$\dot{m}_{\text{stroke}} = \frac{\rho_1(V_1 - V_3)}{\tau} \tag{25}$$

2.4.2 Thermal Efficiency

Based on the schematic from Fig. 5, the thermal efficiency is the ratio of net work output to the heat input through the control volume of the compressor. By dividing Eq. 12 by the total work done by the piston $W = mw$, the equation for thermal efficiency is found by Eq. 26 (2).

$$\eta_T = \frac{W - Q_{loss}}{W} = \frac{m\Delta h}{W} = \frac{\Delta h}{w} \tag{26}$$

This can also be written in terms of the rate of heat loss and compression power as shown by Eq. 27 (2).

$$\eta_T = \frac{\dot{W} - \dot{Q}_{loss}}{\dot{W}} = \frac{\dot{m}\Delta h}{\dot{W}} \tag{27}$$

2.4.3 Mechanical Efficiency

Mechanical efficiency provides an indication of the losses occurring between the piston and driving shaft (2). The following equation is used:

$$\eta_M = \frac{\dot{W}}{P_{in}} \tag{28}$$

where $\dot{W}$ is the compression power from Eq. 10 and P_{in} is the input power from the motor given by Eq. 31 from Appendix A.1.

3 Apparatus and Approach

3.1 Apparatus

In this experiment, the following equipment and tools are used:

- Ingersoll-Rand type 30 Air Compressor model 23 A, shown in Fig. 6;
- Switch board with thermocouple reference junction, AC voltmeter, AC ammeter, Bourdon pressure gauge, engine power calibration chart, voltmete, shown in Fig. 8;
- Set of convergent nozzles with diameters of 0.059", 0.062", 0.078", 0.098", and 0.132";
- LabVIEW software, which acquires data from various sensors, shown in Fig. 7.

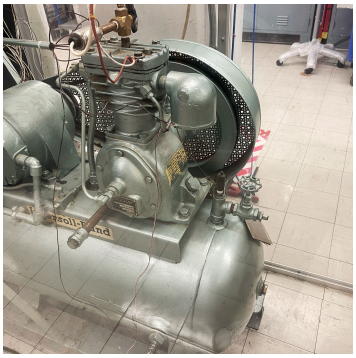

Figure 6: Ingersoll-Rand type 30 Air Compressor model 23A

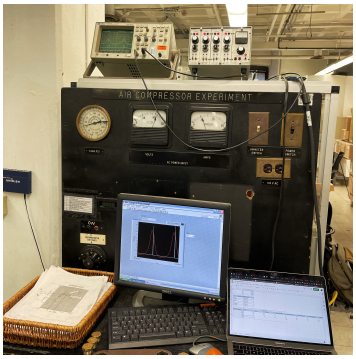

Figure 7: Set up to run the experiment. Oscilloscope and strain gauge conditioner.

Figure 8: Components: AC voltmeter, AC ammeter, ammeter switch.

3.2 Approach

Prior to experimentation, record the pressure and temperature of the ambient environment. Next, calibrate the Vishay strain gauge conditioner. First, power it on and turn the balance knobs until both the "+" and "-" LEDs are nearly darkened. Verify that the gain knob is correctly set. Calibrate the pressure transducer as well. Connect the cylinder to the blue tube and open the valve. Adjust the control pressure to 5psi using the black knob and measure the output voltage using "Air_Comp.vi" in LabVIEW. Continue to calibrate pressure for 10, 15, 20, 30, 40, 50, 60, 70, and 80 psi.

Measure the dimensions of the cylinder head using a caliper before starting. Then begin with the narrowest nozzle, hand-tighten before using the wrench. Check that the enclosure door is fully closed as well as the exhaust valve on top of the tank. Then turn on the power switch, followed by the ammeter switch.

The Vishay LEDs should begin flickering and the oscilloscope should have a signal. At steady state, there should be half-sinusoidal peaks and delta-like pulse spikes. Record the volts and amps from the AC Power Input Unit. To find power, multiply voltage and current and then find this number on the graph provided to find the Power Factor. The y-axis value is then multiplied by the voltage and current to get power.

Flip the thermocouple toggle switch on and then use the decade switch to select the necessary thermocouple. Check all the thermocouples and tank PSI and record at steady state. Open "Air_Comp.vi" in LabVIEW, and set the nozzle size. Press Run, and then save the data. Once the data is saved, turn off the ammeter and power switches and wait for the air tank to bleed off. Only once the pressure gauge has completely become zero, then loosen the nozzle nut with the wrench and repeat the procedure for progressively larger nozzles.

4 Results

4.1 Power Inputs, Outputs, and Other Measured Parameters

Nozzle (in)	Power Input (W)	Power Output (kW)	Power Efficiency
0.059	862.4	357.7	0.536
0.062	828.2	305.8	0.558
0.078	602.8	220.3	0.712
0.098	380.2	110.9	0.961
0.132	0	33.7	N/A

Table 1: Characterization of Power Input and Output from the Motor

Nozzle (in)	$\dot{m}$ (kg/s)	$\dot{m}$ error	$\dot{W}$ (W)	$\dot{Q}$ (W)	η_T	η_M
0.059	$2.25 \cdot 10^{-3}$	$6.07 \cdot 10^{-3}$	410.7	129.0	0.686	0.888
0.062	$2.20 \cdot 10^{-3}$	$5.25 \cdot 10^{-3}$	365.2	86.1	0.764	0.790
0.078	$2.84 \cdot 10^{-3}$	$5.55 \cdot 10^{-3}$	400.2	87.4	0.782	0.933
0.098	$3.00 \cdot 10^{-3}$	$3.93 \cdot 10^{-3}$	280.2	16.2	0.942	0.767
0.132	$3.22 \cdot 10^{-3}$	$2.48 \cdot 10^{-3}$	125.1	-71.3	1.57	N/A

Table 2: Key Parameters of Thermodynamic Cycle of Each Nozzle

4.2 Real Thermodynamic Cycle Data

State	Pressure (kPa)	Volume (m^3)	Temperature (K)	Mass (kg)	Density (kg/m^3)
1	18.6108	0.00032843	303.0000	0.000070275	1.21271
2	429.8914	0.00020388	4344.7746	0.000070275	0.34469
3	499.5349	0.00012885	1347.6534	0.000166383	1.29131
4	75.9159	0.00000815	12.9604	0.000166383	20.40595

Table 3: Real Thermodynamic Cycle for 0.059" Nozzle

State	Pressure (kPa)	Volume (m^3)	Temperature (K)	Mass (kg)	Density (kg/m^3)
1	126.3664	0.00031258	303.0000	0.00045415	1.2127
2	447.1651	0.00031745	1088.8996	0.00045415	1.4306
3	-3.8725	0.00000969	-0.5849	0.00022342	23.0660
4	-3.8725	0.00002279	-1.3764	0.00022342	9.8013

Table 4: Real Thermodynamic Cycle for 0.062" Nozzle

State	Pressure (kPa)	Volume (m^3)	Temperature (K)	Mass (kg)	Density (kg/m^3)
1	36.7072	0.00032843	306.0000	0.00013725	1.2081
2	267.5727	0.00026883	1825.7839	0.00013725	0.5105
3	345.7160	0.00018553	1385.0325	0.00016133	0.8696
4	33.6912	0.00000969	7.0466	0.00016133	16.6564

Table 5: Real Thermodynamic Cycle for 0.078" Nozzle

State	Pressure (kPa)	Volume (m^3)	Temperature (K)	Mass (kg)	Density (kg/m^3)
1	8.4659	0.00032843	307.0000	0.000031551	1.2127
2	231.3800	0.00015108	3859.6626	0.000031551	0.2088
3	162.8332	0.00005370	107.4784	0.000283427	5.2779
4	30.6751	0.00000969	3.6520	0.000283427	29.2614

Table 6: Real Thermodynamic Cycle for 0.098" Nozzle

State	Pressure (kPa)	Volume (m^3)	Temperature (K)	Mass (kg)	Density (kg/m^3)
1	1.6113	0.00032042	305.0000	0.0000058970	1.2081
2	123.0761	0.00025422	18483.7828	0.0000058970	0.0232
3	7.3692	0.00001835	1.4186	0.0003320761	18.0966
4	4.3531	0.00000969	0.4423	0.0003320761	34.2840

Table 7: Real Thermodynamic Cycle for 0.132" Nozzle

Results are tabulated in Table 1 through Table 7. The values in Table 1 were caluclated using measurements from the voltage and current in the air compressor when it was turned on and actively compressing air. The values in Table 2 were calculated using Eq. 5, Eq. 10, Eq. 16, Eq. 26, and Eq. 28. The values in Table 3 through Table 7 were calculated using the raw data from the gauge readings of the air compressor tank and using the Ideal Gas Law.

5 Discussion

By simply comparing the real P-V diagrams in Figures 10-14 to the ideal thermodynamic cycle in Figure 3, there are clear differences. None of the real thermodynamic cycle data

follows the pattern of an ideal thermodynamic cycle, most likely due to different factors in the environment and experimental setup. It is likely that the presence of entropy - something that is not accounted for in ideal thermodynamic cycles - greatly affected the measured values in the experiment. Because the real data does not resemble the ideal cycle, it results in the different analyzed values in the real thermodynamic cycles in Tables 3-7 greatly differing from the expected ideal in Tables 8-12.

This highlights how different stages within the compression cycle are irreversible in actuality when compared to the ideal thermodynamic cycle. Given the compression and expansion data gathered the stages 1-2 and 3-4 can be modelled as a polytropic process, through manipulation of the $PV^n = c$ equation.

The clearance ratio determined by the equation 18, much like other parameters that were analyzed, had a significant difference from that of the ideal thermodynamic cycle. Where the volumes within the stages corresponding to equation 18 allotted for a lower ratio.

Between the different nozzles, it can be seen in Table 1 that as nozzle size increases, generally both power input and output decrease. However, in contrast, power efficiency increases, because input decreases significantly faster than output. Additionally, along with the increase of nozzle size, in Table 2 the value of the mass flow rate, $\dot{m}$, also increases. This is reasonable as the nozzle openings are getting larger so logically more mass should flow. Other parameters that seem to clearly change with nozzle size are heat flow per unit mass, $\dot{Q}$, and thermal efficiency, η_T, where heat per unit mass, $\dot{Q}$, decreases and thermal efficiency, η_T, increases with the increase in nozzle size. It seems that the work input per unit mass, $\dot{W}$, and mechanical efficiency, η_M, both decrease with nozzle size, however it is less clear as there is less consistent of a pattern compared to other parameters.

5.1 Uncertainty

For this experiment, to calculate the uncertainty of the mass flow rate, the partial derivative uncertainty propagation method was used. This means that for some value $F = f(a, b, ..., n)$, the uncertainty is:

$$\sigma_F = \sqrt{\left(\frac{\delta F}{\delta a}\right)^2 \sigma_a^2 + \left(\frac{\delta F}{\delta b}\right)^2 \sigma_b^2 + ... + \left(\frac{\delta F}{\delta n}\right)^2 \sigma_n^2} \tag{29}$$

For this specific experiment, because all mass flow rates were choked, we can use Equations 5 and 29 to get the following equation for the uncertainty of mass flow rate:

$$\sigma_{\dot{m}} = \sqrt{\left(\frac{\dot{m}\sigma_{p_R}}{p_R}\right)^2 + \left(\frac{1}{2}\frac{\dot{m}\sigma_{T_R}}{T_R}\right)^2} \tag{30}$$

Noting that the variables of uncertainty in these derivations are the pressure within the reservoir and temperature within the reservoir.

If the experiment were to be repeated, it would be useful to establish a set of criteria to determine when steady-state is reached by the air compressor. The data's inconsistencies

may in part be due to the lack of consistency in how steady-state conditions were determined for the different nozzles. It is unlikely that leftover pressure from prior experimental runs affected the data because the metric used to determine the complete elimination of built-up pressure - the tank pressure gauge reading 0 psi - was consistently applied both for safety reasons and because of the simplicity of the metric. However, inconsistencies in how tight the nozzles were put on the air compressor may have also contributed to the errors found in the mass flow rates; different team members placed the different nozzles on the air compressor which means that they were likely tightened inconsistently. Additionally, there was no numeric or objective metric employed to determine that a uniform "tightness" was used to fasten and secure each nozzle on the air compressor.

The uncertainty found in $\dot{m}$ for each nozzle, shown in Table 2, is not reasonable. In comparison to the actual $\dot{m}$ values, the error values are on the same scale and occasionally larger in value, meaning that there is a large amount of uncertainty in our values. Large variations in the data itself were likely to contribute to these errors. Re-calibration of the air compressor may be necessary for future repetitions of the experiment. Testing the same nozzles on a different air compressor of the same model would be helpful to find the sources of errors.

6 Conclusions

The motivation behind this experiment follows from the usefulness of the delivery of gases at high pressures for example in industrial equipment. In order to study and better understand the theory and principle of air compressors, this investigation looks into characterizing the differences of the actual and ideal thermodynamic cycles of a compressor through the different sized nozzles.

By separating the cycle into its 4 thermodynamic stages and observing the behavior of the pressure volume diagrams for each nozzle size, determinations of the dependence of some parameters on the nozzle size were able to be made. For instance, as nozzle size increased, mass flow rate increased as did thermal efficiency, and mechanical and volumetric efficiency. Some parameters for the most part decreased with the increase in nozzle size such as heat flow, work done per unit mass, and mechanical efficiency.

As previously mentioned, it would be useful to change the procedure to include a pre-defined method of determining whether or not the air compressor has reached steady-state conditions in order to standardize when data was taken relative to when the air compressor was turned on. This can aid in standardizing the results and eliminating potential time-dependencies in the data.

References

[1] J. Naber and J. Johnson, "Ideal Cycle," *ScienceDirect*.

[2] Q. Lin, "Air compressor principle and experiment," 2022.

[3] Q. Lin, "Air compressor laboratory part 1: Description," 2022.

[4] Q. Lin, "Compressible fluid flow basics and supersonic flow demonstration," 2022.

Contributions by section:

- Abstract: Sam, Bruno
- Introduction: Ashton, Bruno
- Theory: Arlene, Axel, Bruno
- Apparatus and Approach: Christine
- Results: Christine, Bruno
- Discussion: Christine, Bruno, Anton
- Conclusions: Bruno, Anton, Axel, Sam
- Appendix: Bruno, Arlene

A Appendix

A.1 Power Calibration Chart

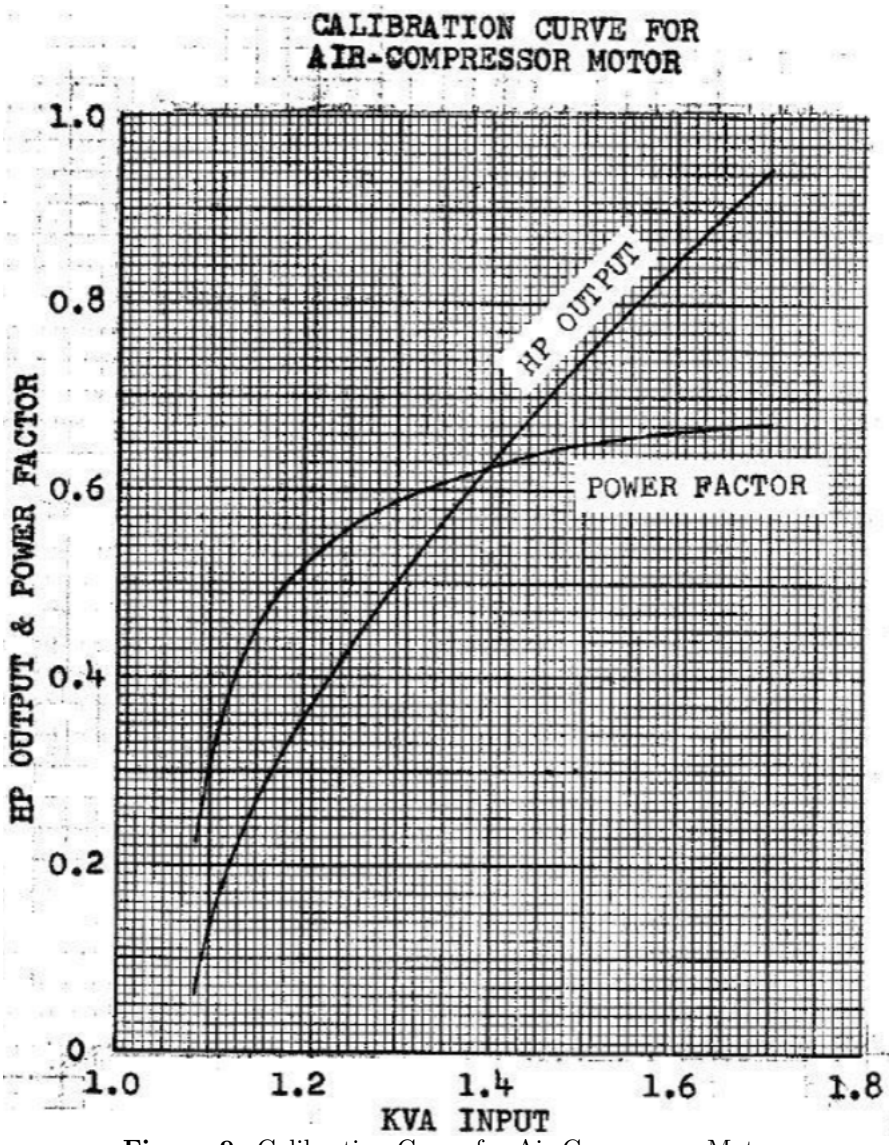

Figure 9: Calibration Curve for Air Compressor Motor

$$P_{in} = (\text{KVA INPUT})(\text{Power Factor}) \tag{31}$$

$$P_{out} = (\text{HP OUTPUT}) \tag{32}$$

$$\eta_{motor} = P_{out}/P_{in} \tag{33}$$

A.2 Idealized Thermodynamic Cycle Data

States	Pressure (kPa)	Temperature (K)	Density (kg/m^3)	Volume (m^3)	Mass (kg)
1	102.2049	293.6000	1.2127	0.00037153	0.00045056
2	550.3639	165.3408	4.0367	0.00011161	0.00045056
3	550.3639	165.3408	4.0367	0.00005299	0.00021390
4	102.2049	293.6000	1.2127	0.00017638	0.00021390

Table 8: Ideal Thermodynamic Cycle for 0.059" Nozzle

States	Pressure (kPa)	Temperature (K)	Density (kg/m^3)	Volume (m^3)	Mass (kg)
1	102.2049	293.6000	1.2127	0.00038093	0.00046196
2	488.3109	159.7850	3.7061	0.00012465	0.00046196
3	488.3109	159.7850	3.7061	0.00006239	0.00023123
4	102.2049	293.6000	1.2127	0.00019067	0.00023123

Table 9: Ideal Thermodynamic Cycle for 0.062" Nozzle

States	Pressure (kPa)	Temperature (K)	Density (kg/m^3)	Volume (m^3)	Mass (kg)
1	102.1250	294.5000	1.2081	0.00036193	0.00043724
2	398.6000	150.6971	3.1954	0.00013683	0.00043724
3	398.6000	150.6971	3.1954	0.00004339	0.00013865
4	102.1250	294.5000	1.2081	0.00011477	0.00013865

Table 10: Ideal Thermodynamic Cycle for 0.078" Nozzle

States	Pressure (kPa)	Temperature (K)	Density (kg/m^3)	Volume (m^3)	Mass (kg)
1	102.2049	293.6000	1.2127	0.00037799	0.00045840
2	267.6789	134.5678	2.4123	0.00019003	0.00045840
3	267.6789	134.5678	2.4123	0.00005945	0.00014342
4	102.2049	293.6000	1.2127	0.00011826	0.00014342

Table 11: Ideal Thermodynamic Cycle for 0.098" Nozzle

States	Pressure (kPa)	Temperature (K)	Density (kg/m^3)	Volume (m^3)	Mass (kg)
1	102.1250	294.5000	1.2081	0.00042585	0.00051446
2	157.2831	115.5361	1.6446	0.00031282	0.00051446
3	157.2831	115.5361	1.6446	0.00010731	0.00017648
4	102.1250	294.5000	1.2081	0.00014609	0.00017648

Table 12: Ideal Thermodynamic Cycle for 0.132" Nozzle

A.3 P-V Diagrams for Different Nozzle Sizes

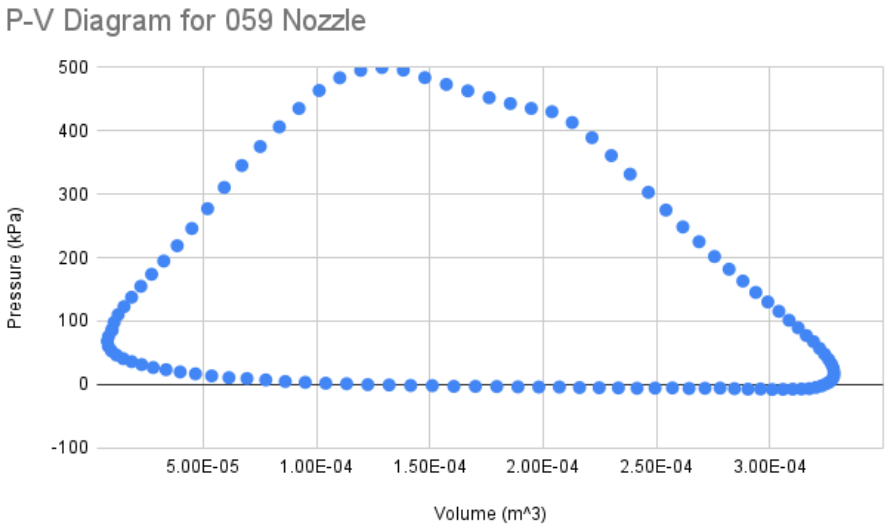

Figure 10: P-V Diagram for 0.059" Nozzle

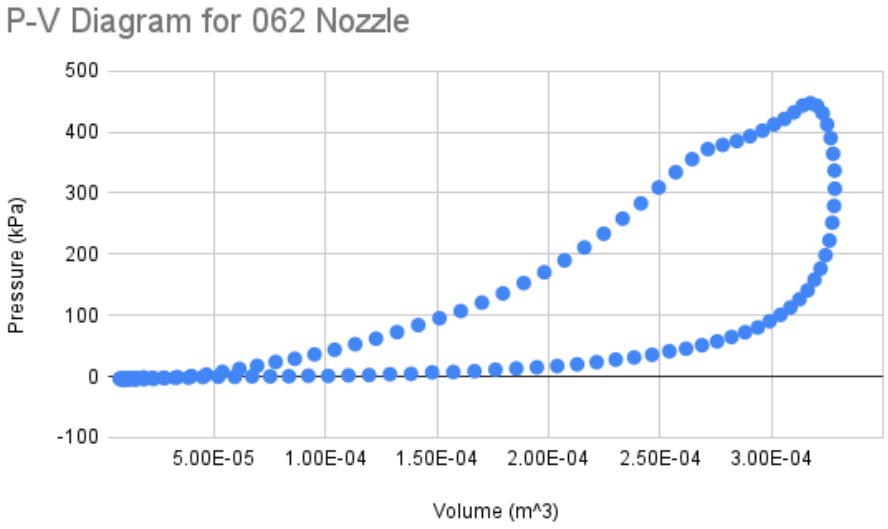

Figure 11: P-V Diagram for 0.062" Nozzle

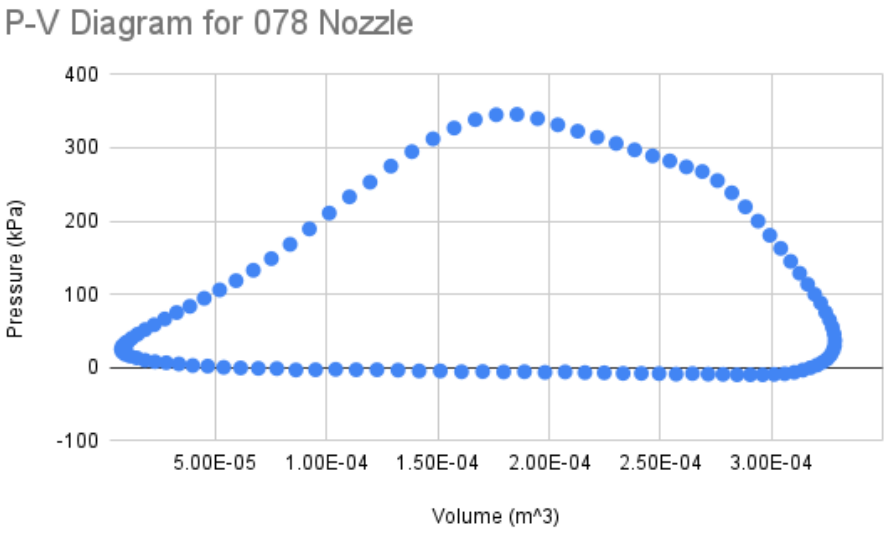

Figure 12: P-V Diagram for 0.062" Nozzle

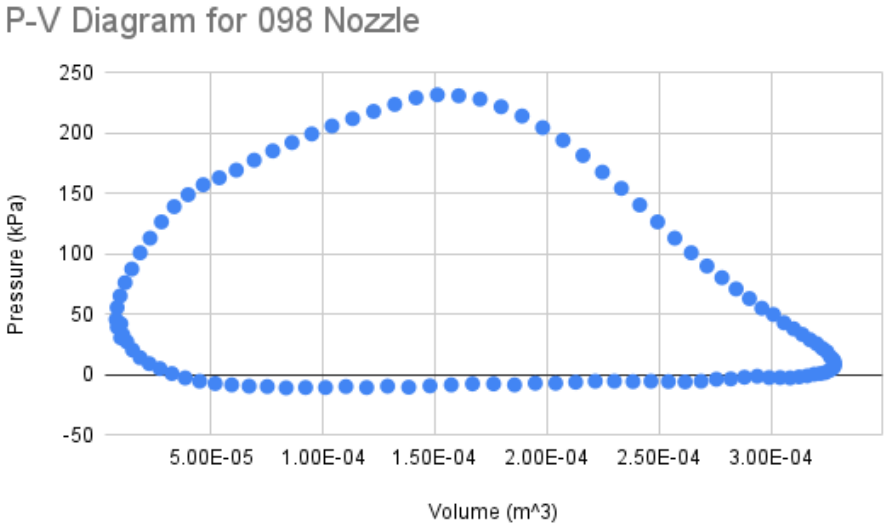

Figure 13: P-V Diagram for 0.098" Nozzle

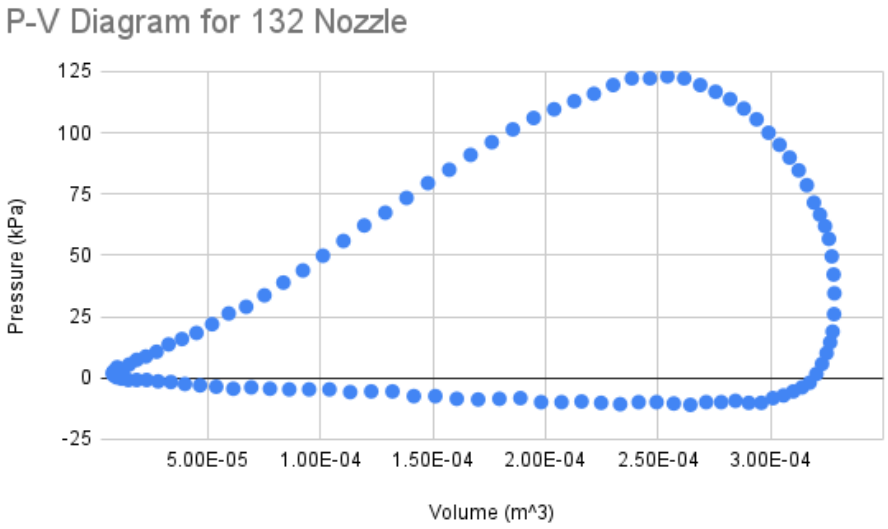

Figure 14: P-V Diagram for 0.132" Nozzle